Catalysis Communications 146 (2020) 106125

Contents lists available at ScienceDirect

Catalysis Communications

journal homepage: www.elsevier.com/locate/catcom

Short communication

Fast CO_2 hydrogenation to formic acid catalyzed by an Ir(PSiP) pincer hydride in a DMSO/water/ionic liquid solvent system

Rodrigo Webber[a], Muhammad I. Qadir[a,1], Eduardo Sola[b,*], Marta Martín[b], Elizabeth Suárez[b], Jairton Dupont[a,*]

[a] Institute of Chemistry, UFRGS, Bento Gonçalves, 9500, Porto Alegre 91501-970, Rio Grande do Sul, Brazil
[b] Instituto de Síntesis Química y Catálisis Homogénea (ISQCH), CSIC-Universidad de Zaragoza, 50009, Spain

ARTICLE INFO

Keywords:
Ionic liquids
CO_2 hydrogenation
Formic acid
Iridium
Solvent-cage

ABSTRACT

Complex [IrClH{κP,P,Si-Si(Me)(C_6H_4–2-P*i*Pr_2)$_2$}] (**1**) showed a remarkable catalytic activity for CO_2 hydrogenation in a DMSO/H_2O solvent system incorporating 1,2-dimethyl-3-butylimidazolium acetate ionic liquid (IL), producing 0.94 M formic acid with initial TOFs up to 1432 h^{-1} (CO_2/H_2 = 20/40 bar, 30 °C). While the hydrogenation outcome followed dependences upon gas composition, pressure and temperature similar to those of other efficient systems in DMSO/H_2O, the kinetic dependence upon catalyst loading revealed non-linear effects suggestive of relevant IL-catalyst interactions. NMR speciation studies identified two major complexes, [Ir(OCHO)(H){κ*P*,*P*,Si-Si(Me)(C_6H_4–2-P*i*Pr_2)$_2$}] (**2**) and [Ir(H)$_2${κP,P,Si-Si(Me)(C_6H_4–2-P*i*Pr_2)$_2$}(DMSO)] (**3**), potentially responsible for catalytic cycling though inactive outside the current solvent system.

1. Introduction

Imidazolium-based ionic liquids (ILs) can form solvent "cages" around catalysts (enzymes, nanoparticles or complexes), creating ionic nano-container environments that control diffusion of reagents, intermediates and products, to or from the active sites, through their hydrophobicity and contact ion pairs [1,2]. Such a scenario is akin to that of micelle nano (micro)reactors, which compartmentalize and concentrate/separate reagents thereby altering the apparent reaction rates and equilibrium constants [3]. Cage effects were already demonstrated for catalytic reactions in both bare ILs and hybrid solvents containing ILs [4]. In particular, the hydrogenation of carbon dioxide (CO_2) to free formic acid (FA) catalyzed by either transition metal complexes or nanoparticles in ILs/DMSO/water solutions was proposed to involve such micelle nanoreactors [5,6].

Due to its potential significance to the production of C1 feedstocks and fuels, CO_2 hydrogenation is among the most investigated transition metal-catalyzed reactions, though processes are commonly designed to afford formates and no free FA [7]. Addition of base is required to achieve favorable thermodynamics, and is also thought to be kinetically relevant for assisting the heterolytic cleavage of hydrogen within catalytic cycles [8]. Interestingly, recent evidence suggests that inside ILs solvent cages these roles can be efficiently and more simply taken on by basic IL counter-anions such as acetate, which generate buffer-like local environments that modify concentrations and equilibria among the species involved in the reactions with CO_2 [9].

Aimed at further substantiating such IL-solvent-cage effects, this work investigates the performance of the five-coordinate PSiP pincer complex [IrClH{κP,P,Si-Si(Me)(C_6H_4–2-P*i*Pr_2)$_2$}] (**1**) (Fig. 1) in the catalytic hydrogenation of CO_2 to FA. To the frequent success of pincer type iridium complexes in this reaction [10–13], this catalyst candidate adds on a rich hydride chemistry that has been already investigated in part [14,15]. We show herein that the catalyst achieved 0.94 M FA with initial turnover frequencies up to 1432 h^{-1} when the CO_2 hydrogenation is performed at 30 °C in a mixture of 1,2-dimethyl-3-butylimidazolium acetate (BMMIm.OAc) IL/DMSO/water, thus demonstrating the fastest production of free FA until now.

2. Results and discussion

Complex **1** was examined for the catalytic hydrogenation of CO_2 to FA in ILs/DMSO/H_2O solutions. DMSO was used because of its intermolecular hydrogen bonding interactions with imidazolium-based ILs, previously recognized to result into a loose packing of the constituents of the mixture [16]. No FA was produced when 1,2-dimethyl-3-butylimidazolium tetrafluoroborate (BMMIm.BF_4) was used as the IL,

* Corresponding authors.
E-mail addresses: sola@unizar.es (E. Sola), jairton.dupont@ufrgs.br (J. Dupont).
[1] Current address: Department of Nanocatalysis, J. Heyrovský Institute of Physical Chemistry, Dolejškova 2155/3, 18223 Prague 8, Czech Republic.

https://doi.org/10.1016/j.catcom.2020.106125
Received 15 May 2020; Received in revised form 25 July 2020; Accepted 27 July 2020
Available online 31 July 2020

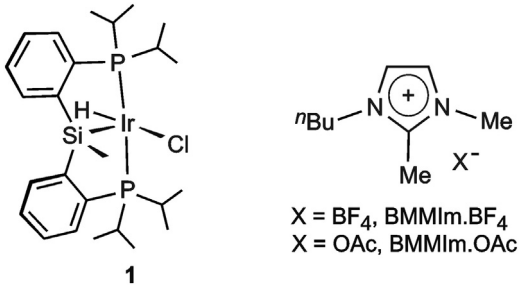

Fig. 1. Structures of the catalyst precursor [IrClH{κP,P,Si-Si(Me)(C_6H_4–2-P*i*Pr$_2$)$_2$}] (**1**) and the ILs (BMMIm.BF_4 and BMMIm.OAc) used in this study.

Table 1
Catalytic hydrogenation of CO_2 to FA by Ir complex **1**.[a]

Entry	Media	FA (mmol)	[FA] (mol L^{-1})[b]	TON
1[c]	DMSO	–	–	–
2	BMMIm.BF_4/DMSO	–	–	–
3	BMMIm.OAc/DMSO	3.96	0.94	2475
4[d]	BMMIm.OAc/DMSO	2.88	0.67	1800
5[e]	BMMIm.OAc/H_2O	–		–
6[e,f]	NaOAc/H_2O	–		–

[a] Reaction conditions: **1** (1.6 μmol), IL (200 mg), DMSO (4.35 g), CO_2/H_2 (1:2, 60 bar), *T* (30 °C), reaction time 18 h.
[b] Total reaction volume was calculated at initial composition, assuming additive volumes.
[c] no IL.
[d] H_20 (200 mg).
[e] no DMSO, H_2O (4.35 g).
[f] no IL, NaOAc (82 mg).

whereas in solutions containing 1,2-dimethyl-3-butylimidazolium acetate (BMMIm.OAc) **1** showed remarkable catalytic activity (Table 1, entries 2 and 3). The difference between ILs confirms the acetate anion buffering properties as crucial for the stabilization of weak carbonic acid species [17]. Reactions containing acetate but not IL were found non-productive either (Table 1, entry 6).

A controlled small amount of water (100 mg) was added to the solvent mixture since it was expected to benefit catalysis in various ways: *i*) it may accelerate the reaction because of its combination with CO_2 to form bicarbonate [17] *ii*) together with DMSO it may afford a solvent system able to stabilize the free FA product through H-bonding [18], and *iii*) it may strongly influence structural organization and electronic properties of imidazolium based ILs [19]. Still, on increasing this amount of added water to 200 mg the yield of FA dropped, eventually turning zero in the absence of DMSO (Table 1, entries 4 and 5).

Fig. 2(a) illustrates the time progress of a hydrogenation reaction under the standard experimental conditions detailed in Table 1, entry 3. The concentration of FA achieved in 1 h was already as high as 0.55 M (1432 TON), reaching the value of 0.94 M (2475 TON) after a 18 h reaction period. Attending to the shape of the FA production curve, this latter concentration value is close to the maximum (equilibrium) yield of the system, and compares well with the reported outcome of other efficient catalysts in DMSO-based solvent systems [5,18,20,21]. Notably, the initial TOF value, 1432 h^{-1}, is well above the maximum registered in these precedents, making this catalyst system the fastest among the most efficient in the production of free FA reported so far.

Despite being certainly homogeneous, the reaction evidenced non-linear catalyst concentration effects that could tentatively be attributed to the aforementioned expected solvent organization in cages. The Fig. 2(b) displays the yields of FA obtained using four different catalyst loadings, under otherwise equal solvent and reagent compositions, and the same reaction time. The experiment using 1.6 μmol of **1**, which corresponds to the efficient system already discussed upon Table 1, entry 3 and Fig. 2(a), clearly outperforms the other three, which among themselves display approximately linear yield increments and similar TONs, as expected for a homogeneous system. Since the variables defining reaction thermodynamics remain the same in the four experiments, differences must be of kinetic origin. This points to the possible IL-catalyst interaction as crucial not only to enable catalysis, as inferred from the various void entries of Table 1, but also to achieve optimum kinetics. In this respect, it seems conceivable that the solvent system could contribute to CO_2 and H_2 pre-organization at catalytic sites in the same way than other successful outer-sphere strategies do, such as those based on ligand scaffolds with appended lone pairs or H-bonding sites [22–25].

The hydrogenation yield was also studied at different compositions and pressures of the CO_2/H_2 gas mixture, and different temperatures. Fig. 3 collects FA concentration values obtained after 18 h of reaction (that is, at equilibrium or close to it) that reproduce the trends reported for other DMSO/water systems [5,18,20,21]. For CO_2/H_2 (1:2) mixtures, going from 10 to 60 bar led to a clear productivity increase (Fig. 3(a)), while gas compositions poorer in H_2 consistently led to lower yields. Besides the anticipated increase in solubility of each individual gaseous reagent with increasing pressure [26], their mutual miscibility in the liquid phase is expected to further increment their concentrations. No CO was detected in the gas phase at temperatures below 80 °C, which rules out FA degradation under reaction conditions. The inverse dependence of the FA yield upon temperature (Fig. 3(b)) is also a common observation in DMSO/water mixtures [5,20], and corresponds to that qualitatively expected from the equilibrium entropy and solubility considerations.

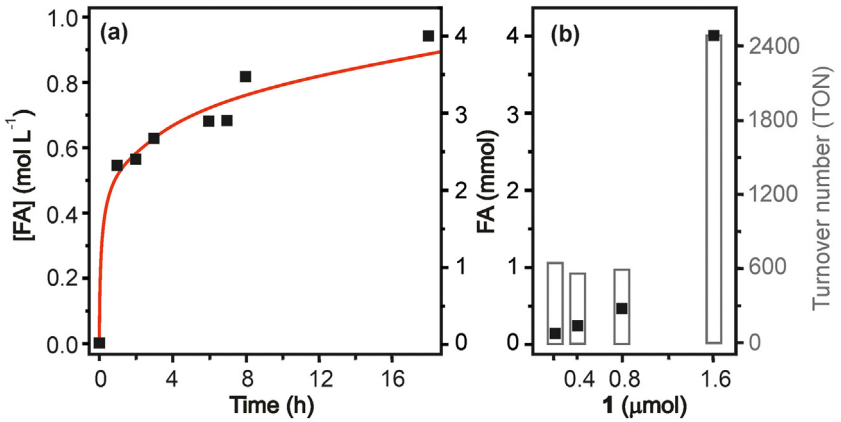

Fig. 2. (a) Catalytic hydrogenation of CO_2 to FA vs. time using BMMIm.OAc as IL and 1.6 μmol of catalyst precursor **1**. (b) Effect of catalyst precursor loading in the yield (■) and TON (bars) of this reaction at 18 h reaction time. Conditions: DMSO (4.35 g), BMMIm.OAc (200 mg), CO_2/H_2 (1:2, 60 bar), *T* (30 °C).

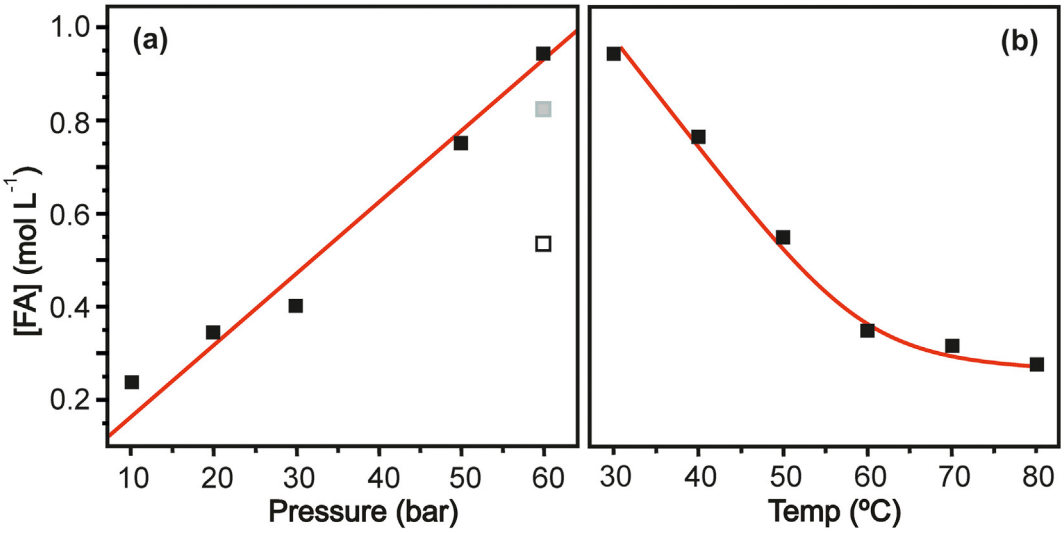

Fig. 3. Hydrogenation yields estimated at 18 h reaction time: (a) at 30 °C under different total pressures and compositions of the CO_2/H_2 gas mixture: ■ (1:2), ■ (1:1), ▢ (2:1). (b) at different temperatures under 60 bar of CO_2/H_2 (1:2). Conditions: DMSO (4.35 g), BMMIm.OAc (200 mg).

2.1. Catalytic intermediate complexes

The solutions of catalyst precursor **1** in DMSO-d_6 displayed NMR spectra significantly different from those recorded in C_6D_6 or $CDCl_3$, suggesting that in DMSO-d_6 **1** is in equilibrium with the cationic monohydride that results after chloride displacement by two molecules of the coordinating solvent, just as observed for acetonitrile or water [14]. Thus, the characteristic ^{1}H NMR triplet at about δ −24 ppm (J_{HP} = 14 Hz) in non-coordinating solvents broadens and shifts to δ − 18.34 in DMSO-d_6 at room temperature (Fig. 4). Such hydride signal was not visible in the ^{1}H NMR spectra recorded for **1** in the actual catalytic solvent mixture (BMMIm.OAc/DMSO/D_2O) under CO_2/H_2 pressure (1:1, 40 bar), which in turn showed numerous hydride resonances evidencing an intricate catalyst speciation (Fig. 4). At least in part, the presence of that many species could again be attributed to the high organization of the reaction media, which can offer to the hydrides a variety of potential supramolecular interactions that may shift the ^{1}H NMR hydride signals in multiple ways. Yet, the major resonances of the spectrum: a triplet at δ − 27.78 (J_{HP} = 12 Hz), and two apparent triplets at δ − 9.96 and − 13.00 could be identified as corresponding to complexes [Ir(OCHO)(H){κ*P*,*P*,Si-Si(Me)(C_6H_4–2-P*i*Pr_2)$_2$}] (**2**) and [Ir(H)$_2${κP,P,Si-Si(Me)(C_6H_4–2-P*i*Pr_2)$_2$}(DMSO)] (**3**), respectively, which were independently generated and characterized from **1** and reagents present in the actual catalytic reaction, as shown in Scheme 1.

The reaction between **1** and sodium formate in DMSO-d_6 directly led to dihydride **3**, likely after replacement of the chloride ligand with the formate, followed by CO_2 deinsertion. Accordingly, the corresponding reaction with potassium acetate gave the acetato-hydrido complex [Ir(OCMeO)(H){κ*P*,*P*,Si-Si(Me)(C_6H_4–2-P*i*Pr_2)$_2$}] (**4**), while the use of deuterated sodium formate gave an isotopologue of **3** selectively

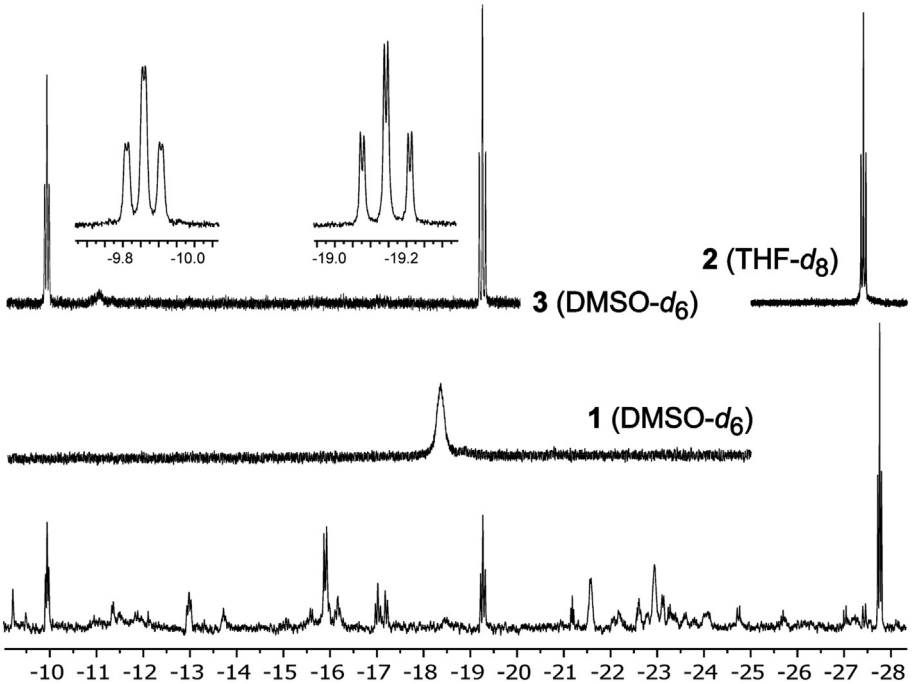

Fig. 4. Comparison among the hydride regions of the ^{1}H NMR spectrum recorded under catalytic conditions (below) and those of the catalyst precursor and possible catalytic intermediates.

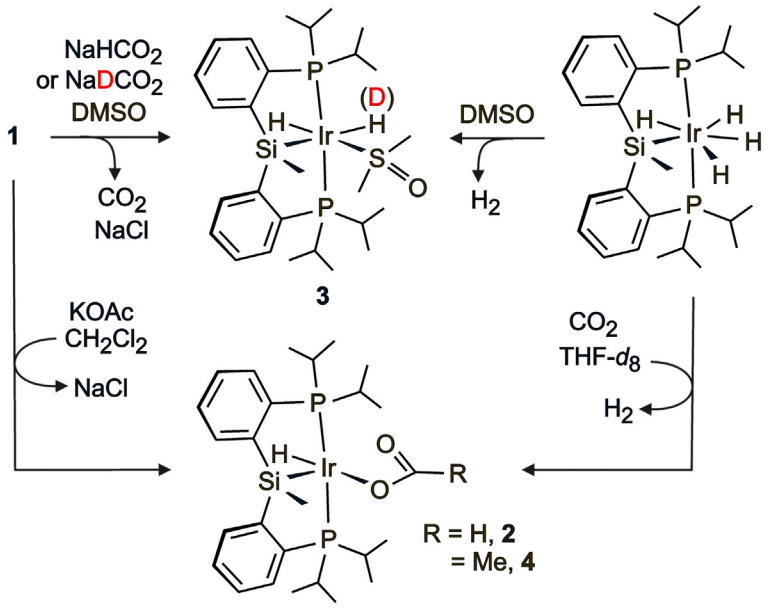

Scheme 1. Synthesis of putative reaction intermediates **2** and **3**. For discussions on the coordination modes of DMSO and formate/acetate ligands, see Experimental Section.

deuterated at the hydride ligand *trans* to silicon.

Complex **3** could also be generated from the known tetrahydrido complex [Ir(H)$_4${κ*P*,*P*,Si-Si(Me)(C$_6$H$_4$–2-P*i*Pr$_2$)$_2$}] in DMSO as solvent, after the simple release of H_2. These reactions indicate that in this solvent and without CO_2 pressure, the possible equilibrium between **2** and **3** is shifted to the dihydride. In contrast, reaction of the tetrahydrido complex and CO_2 excess in less coordinating solvents such as THF-d_8 quantitatively afforded the hydrido-formato complex **2**, demonstrating the feasibility of CO_2 insertion into the Ir − H bond. Like the parent acetato complex **4** and analogues containing O-donor anionic ligands such as triflate, **2** shows a characteristic ^{1}H NMR hydride chemical shift that is significantly lower than those typical for other Ir (PSiP) hydrides [14,27].

Generally accepted mechanisms for homogeneous CO_2 hydrogenation feature hydride complexes capable of inserting this reagent to yield formate intermediates, which in turn are able to split the hydrogen molecule yielding FA (or formate in the presence of base) and regenerating the initial hydride [13]. In our case, the cycling between complexes **3** and **2**, respectively, can satisfy such a scheme. Yet, our experiments also indicate that reaction of **2** with H_2 to form **3** and FA does not progress at all in conventional organic solvents, a fact that highlights the essential role played by the current solvent system.

3. Conclusions

In conventional organic solvents, the Ir(PSiP) pincer complex **1** is inactive for the catalytic hydrogenation of CO_2 to FA, but turns very efficient in IL/DMSO/H_2O mixtures containing acetate counter-anions. The efficiency is both kinetic, with unprecedented TOFs above 1400 h^{-1}, and thermodynamic, affording high equilibrium FA concentrations similar to other successful catalytic systems in DMSO/water. As in parent catalytic systems, the switch to activity can be in part attributed to the basic acetate, which buffers the solutions to turn FA production spontaneous. Yet, a relevant kinetic role of the IL is also inferred from the absence of catalytic activity in other media and the observed non-linear catalyst concentration effects, which point to the, previously substantiated, IL-induced solvent organization in cages containing the catalyst as potentially crucial. The catalyst speciation studies identified hydrido-formate and dihydrido possible intermediate complexes that turned out to be non-connectable outside the current solvent system: again suggesting that IL-catalyst interactions could play an essential role. Further kinetic and characterization studies aimed at identifying such interactions are in progress.

4. Experimental section

4.1. Catalytic CO_2 hydrogenation to formic acid

ILs, BMMIm.OAc (1,2-dimethyl-3-butylimidazolium acetate) and BMMIm.BF_4 (1,2-dimethyl-3-butylimidazolium tetrafloroborate), were prepared via reported methods [28]. DMSO was purchased from Sigma-Aldrich chemicals. CO_2 (> 99.999%) and H_2 (> 99.999%) were purchased from White-Martins Ltd., Brazil. Reactions were performed in a Parr multiple reactors system (100 mL). Typically, an aliquot of a 16.0 mM solution of **1** in DMSO was added under argon atmosphere to a solution containing BMMIm.OAc (200 mg, 0.94 mmol), DMSO (3.95 mL, 4.35 g, 51 mmol) and H_2O (100 mg, 5.6 mmol). The mixture was heated at the desired temperature, and the argon in the reactor was removed by passing hydrogen gas. Then, the reactor was filled with CO_2/H_2 at the desired pressure from a mixture previously prepared in an independent stainless steel Parr reservoir. After closing the connection to the reservoir, the reaction was stirred at 500 rpm for the desired reaction time. Pressure drop inside reactor during reactions was typically below 5% and was not taken into account. The reactor was cooled in an ice-cooled water bath and gases were carefully vented. An aliquot of the reaction mixture dissolved in DMSO-d_6 was used to determine the yield in FA by ^{1}H NMR using the IL as internal standard. The gaseous products were analysed by gas chromatography (GC) Agilent 6820 equipped with a Porapak Q 80–100 mesh column and argon as the carrier gas. The kinetic profile of Fig. 2(a) corresponds to a series of experiments stopped at different reaction times. In general, the FA yield data are the mean value of at least two independent experiments.

4.2. Preparation and characterization of the new complexes

The synthesis of the complexes was carried out with exclusion of air by using standard Schlenk techniques or in an argon-filled glovebox (MBraun). DMSO was purchased from Sigma-Aldrich chemicals and dried over 3 Å molecular sieves. Other solvents were obtained from a

solvent purification system (MBraun). Deuterated solvents were dried with appropriate drying agents and degassed with argon prior to use. All other reagents were commercial and were used as received. Precursor **1** and the tetrahydrido complex [Ir(H)$_4${κ*P,P,Si*-Si(Me)(C$_6$H$_4$–2-*Pi*Pr$_2$)$_2$}] were prepared as previously described [14,15].

C, H and N analyses were carried out in a Perkin-Elmer 2400 CHNS/O analyser. MALDI-TOF MS were obtained in a Bruker Microflex mass spectrometer using DCTB (1,1-dicyano-4-terbuthylphenyl-3-methylbutadiene) as matrix. Attenuated total reflection infrared spectra (ATR-IR) of solid samples were run on a Perkin-Elmer Spectrum 100 FT-IR spectrometer. NMR spectra were recorded on Bruker Avance 400 MHz spectrometer. ^{1}H (400.13 MHz) and ^{13}C (100.6 MHz) NMR chemical shifts were measured relative to partially deuterated solvent peaks but are reported in ppm relative to TMS. ^{19}F (376.5 MHz), ^{31}P (162.0 MHz) and ^{29}Si (79.5 MHz) chemical shifts were measured relative to $CFCl_3$, H_3PO_4 (85%) and TMS, respectively. Coupling constants, ^nJ and $^{n,m}N$ (= ^nJ + $^mJ'$ for couplings with chemically equivalent but magnetically inequivalent nuclei), are given in hertz. In general, NMR spectral assignments were achieved through ^{1}H{^{1}H}, ^{1}H cosy, ^{1}H nOesy, ^{1}H{^{31}P}, ^{13}C apt, and ^{1}H/^{13}C hsqc experiments. Unless otherwise indicated, the NMR data are given at room temperature.

4.2.1. [Ir(OCHO)H{κ*P,P,Si*-Si(Me)(C$_6$H$_4$–2-*Pi*Pr$_2$)$_2$}] (2)

A solution of [Ir(H)$_4${κ*P,P,Si*-Si(Me)(C$_6$H$_4$–2-*Pi*Pr$_2$)$_2$}] (30.0 mg, 0.048 mmol) in 0.5 mL of THF-d_8 contained in a PTFE-valved NMR tube was frozen. The argon inside the tube was evacuated, and the tube was filled with CO_2 (ca. 1 bar) and sealed. The resulting yellow solution was analysed by NMR and found to contain **2** as the major reaction product (> 90%), together with unreacted tetrahydrido precursor and dissolved H_2. The attempts to isolate **2** from this solution gave mixtures of compounds. ^{1}H NMR (THF-d_8): δ −27.40 (td, $^2J_{HP}$ = 15.8, $^4J_{HH}$ = 1.2, 1H, IrH), 0.36 (s, 3H, SiCH$_3$), 0.86 (dvt, $^3J_{HH}$ = 8.1, $^{3,5}N_{HP}$ = 15.3, 6H, PCHC*H*$_3$), 1.10 (dvt, $^3J_{HH}$ = 8.9, $^{3,5}N_{HP}$ = 16.5, 6H, PCHC*H*$_3$), 1.23 (dvt, $^3J_{HH}$ = 6.1, $^{3,5}N_{HP}$ = 13.0, 6H, PCHC*H*$_3$), 1.36 (dvt, $^3J_{HH}$ = 8.5, $^{3,5}N_{HP}$ = 15.7, 6H, PCHC*H*$_3$), 2.52, 3.01 (both m, 2H each, PC*H*CH$_3$), 7.28, 7.36 (both ddvt, $^3J_{HH}$ ≈ 7.5, $^3J_{HH'}$ ≈ 7.1, $^{5,6}N_{HP}$ = 2.2, 2H each, CH), 7.63 (dvt, $^3J_{HH}$ = 7.7, $^{3,5}N_{HP}$ = 7.1, 2H, CH), 8.06 (d, $^3J_{HH'}$ ≈ 7.1, 2H, CH), 9.21 (td, $^2J_{HP}$ = 1.3, $^4J_{HH}$ = 1.2, 1H, O$_2$CH). ^{31}P{^{1}H} NMR (THF-d_8): δ 60.42 (s). ^{13}C{^{1}H} NMR (THF-d_8): δ 3.19 (s, SiCH$_3$), 18.06 (s, PCH*C*H$_3$), 18.68 (vt, $^{2,4}N_{CP}$ = 5.7, PCH*C*H$_3$), 20.09 (vt, $^{2,4}N_{CP}$ = 4.5, PCH*C*H$_3$), 20.69 (s, PCH*C*H$_3$), 26.65 (vt, $^{1,3}N_{CP}$ = 23.8, P*C*HCH$_3$), 26.93 (vt, $^{1,3}N_{CP}$ = 31.9, P*C*HCH$_3$), 128.07 (vt, $^{4,5}N_{CP}$ = 7.1, CH), 129.99 (s, CH), 131.00 (vt, $^{3,4}N_{CP}$ = 4.7, CH), 132.56 (vt, $^{3,4}N_{CP}$ = 18.4, CH), 142.80 (vt, $^{1,3}N_{CP}$ = 54.4, C), 158.85 (vt, $^{2,3}N_{CP}$ = 42.1, C), 172.17 (s, O$_2$CH). ^{29}Si{^{1}H} NMR (THF-d_8): δ 9.60 (t, $^3J_{SiP}$ = 2.6). The complex is proposed to contain a monodentate κ*O* formato ligand by analogy with previously described complexes containing triflates or acetates [14,27].

4.2.2. [Ir(H)$_2${κ*P,P,Si*-Si(Me)(C$_6$H$_4$–2-*Pi*Pr$_2$)$_2$}{DMSO}] (3)

The compound was generated in solution via two methods: (a) A solution of **1** (20.0 mg, 0.03 mmol) in DMSO-d_6 (0.5 mL) was treated with sodium formate (4.1 mg, 0.06 mmol), and (b) A solution of [Ir(H)$_4${κ*P,P,Si*-Si(Me)(C$_6$H$_4$–2-*Pi*Pr$_2$)$_2$}] (100 mg, 0.16 mmol) in toluene (3 mL) was treated with DMSO (57 μL, 0.8 mmol). The solution was concentrated to dryness and treated with diethyl ether, filtered and again concentrated to dryness to give an off-white solid (88.3 mg). The solid was air sensitive and gave incorrect microanalyses. Its MS spectra just displayed peaks corresponding to a mixture of [IrH(PSiP)]$^+$ and [Ir(PSiP) − H]$^+$ fragments. ^{1}H NMR (C$_6$D$_6$): δ −18.47 (td, $^2J_{HP}$ = 20.0, $^2J_{HH}$ = 2.9, 1H, IrH), −9.46 (td, $^2J_{HP}$ = 14.3, $^2J_{HH}$ = 2.9, 1H, IrH), 0.91 (dvt, $^3J_{HH}$ = 6.7, $^{3,5}N_{HP}$ = 15.7, 6H, PCHC*H*$_3$), 0.83 (dvt, $^3J_{HH}$ = 8.4, $^{3,5}N_{HP}$ = 15.6, 6H, PCHC*H*$_3$), 0.98 (dvt, $^3J_{HH}$ = 6.9, $^{3,5}N_{HP}$ = 12.0, 6H, PCHC*H*$_3$), 1.13 (s, 3H, SiCH$_3$), 1.36 (dvt, $^3J_{HH}$ = 6.7, $^{3,5}N_{HP}$ = 16.1, 6H, PCHC*H*$_3$), 2.33, 2.61 (both m, 2H each, PC*H*CH$_3$), 3.11 (s, 6H, OSCH$_3$), 7.05 (m, 2H, CH), 7.21 (m, 4H, CH), 8.27 (d, $^3J_{HH'}$ ≈ 7.0, 2H, CH). ^{31}P{^{1}H} NMR (C$_6$D$_6$): δ 58.00 (s). ^{13}C{^{1}H} NMR (C$_6$D$_6$): δ 5.05 (s, SiCH$_3$), 15.93 (vt, $^{2,4}N_{CP}$ = 3.7, PCH*C*H$_3$), 18.03 (vt, $^{2,4}N_{CP}$ = 6.2, PCH*C*H$_3$), 19.56 (vt, $^{2,4}N_{CP}$ = 2.4, PCH*C*H$_3$), 20.36 (vt, $^{2,4}N_{CP}$ = 3.6, PCH*C*H$_3$), 22.05 (vt, $^{1,3}N_{CP}$ = 35.6, P*C*HCH$_3$), 25.20 (vt, $^{1,3}N_{CP}$ = 23.9, P*C*HCH$_3$), 58.41 (s, OSCH$_3$), 126.38 (vt, $^{4,5}N_{CP}$ = 7.3, CH), 128.55 (vt, $^{3,5}N_{CP}$ = 6.1, CH), 129.26 (vt, $^{2,4}N_{CP}$ = 1.8, CH), 133.21 (vt, $^{3,4}N_{CP}$ = 18.5, CH), 144.89 (vt, $^{1,3}N_{CP}$ = 57.8, C), 160.78 (vt, $^{2,3}N_{CP}$ = 41.0, C). ^{29}Si{^{1}H} NMR (DMSO-d_6): δ 26.20 (t, $^3J_{SiP}$ = 8.2). The coordination mode of DMSO in the complex is proposed to be κ*S* to better account for the non-lability of the ligand inferred from the ^{1}H NMR spectra in C$_6$D$_6$ in the presence of dissolved DMSO. κ*S* is also the most common coordination mode of DMSO in Ir complexes [29].

4.2.3. Preparation of [Ir{OC(Me)O}(H){κ*P,P,Si*-Si(Me)(C$_6$H$_4$–2-*PiPr$_2$)$_2$}] (4)

A solution of **1** (250 mg, 0.38 mmol) in CH_2Cl_2 (12 mL) was treated with potassium acetate (186 mg, 1.90 mmol). The mixture was stirred at RT for 24 h. The solution was filtered and then concentrated to ca. 0.5 mL and treated with hexane to obtain an off-white solid. The solid was separated by decantation, washed with hexane, and dried in vacuo: yield 220 mg (85%). Anal. Cald. for $C_{27}H_{43}O_2P_2SiIr$: C, 47.56; H, 6.36. Found: C, 47.83; H, 6.54. ^{1}H NMR (C$_6$D$_6$): δ −27.13 (t, $^2J_{HP}$ = 15.9, 1H, IrH), 0.75 (s, 3H, SiCH$_3$), 0.91 (dvt, $^3J_{HH}$ = 6.9, $^{3,5}N_{HP}$ = 15.6, 6H, PCHC*H*$_3$), 1.09 (dvt, $^3J_{HH}$ = 7.2, $^{3,5}N_{HP}$ = 12.9, 6H, PCHC*H*$_3$), 1.25 (dvt, $^3J_{HH}$ = 7.2, $^{3,5}N_{HP}$ = 16.2, 6H, PCHC*H*$_3$), 1.44 (dvt, $^3J_{HH}$ = 6.9, $^{3,5}N_{HP}$ = 15.9, 6H, PCHC*H*$_3$), 1.94 (s, 3H, O$_2$CCH$_3$), 2.47, 2.67 (both m, 2H each, PC*H*CH$_3$), 7.10, 7.21 (both ddvt, $^3J_{HH}$ ≈ 7.8, $^3J_{HH'}$ ≈ 7.2, $^{5,6}N_{HP}$ = 2.7, 2H each, CH), 7.33 (dvt, $^3J_{HH}$ = 7.8, $^{3,5}N_{HP}$ = 6.7, 2H, CH), 8.06 (d, $^3J_{HH'}$ ≈ 7.2, 2H, CH). ^{31}P{^{1}H} NMR (C$_6$D$_6$): δ 60.50 (s). ^{13}C{^{1}H} NMR (C$_6$D$_6$): δ 3.21 (s, SiCH$_3$), 18.02 (s, PCH*C*H$_3$), 18.55 (vt, $^{2,4}N_{CP}$ = 5.9, PCH*C*H$_3$), 19.53 (vt, $^{2,4}N_{CP}$ = 4.8, PCH*C*H$_3$), 20.29 (vt, $^{2,4}N_{CP}$ = 3.1, PCH*C*H$_3$), 25.57 (s, O$_2$C*C*H$_3$), 26.60 (vt, $^{1,3}N_{CP}$ = 31.2, P*C*HCH$_3$), 26.89 (vt, $^{1,3}N_{CP}$ = 23.5, P*C*HCH$_3$), 127.24 (vt, $^{4,5}N_{CP}$ = 7.2, CH), 129.28 (vt, $^{3,5}N_{CP}$ = 2.0, CH), 129.96 (vt, $^{2,4}N_{CP}$ = 5.4, CH), 132.07 (vt, $^{3,4}N_{CP}$ = 18.4, CH), 143.15 (vt, $^{1,3}N_{CP}$ = 54.6, C), 158.74 (vt, $^{2,3}N_{CP}$ = 42.3, C), 181.83 (s, O$_2$*C*CH$_3$). ^{29}Si{^{1}H} NMR (C$_6$D$_6$): δ 11.73 (t, $^3J_{SiP}$ = 3.0). As explained for **2**, complex **4** is proposed to contain a monodentate κ*O* acetate ligand. In this case, the proposal is further supported by the two ν(OCO) modes found in the IR spectrum, at 1567 and 1444 cm^{-1} [30].

Declaration of Competing Interest

The authors declare that they have no known competing financial interests or personal relationships that could have appeared to influence the work reported in this paper.

Acknowledgements

The authors are thankful for financial support from CAPES (158804/2017-01 and 001), FAPERGS (16/2552-0000 and 18/2551-0000561-4), CNPq (406260/2018-4, 406750/2016-5 and 465454/2014-3), MINECO/Fondo Europeo de Desarrollo Regional (CTQ2015-64486-R) and Gobierno de Aragón/FEDER (E08-17R). E. Suárez is grateful to MINECO for a FPI fellowship (BES2013-063359). M. I. Qadir also acknowledges support from the European Union's Horizon 2020 research and innovation program under grant agreement no. 810310, which corresponds to the J. Heyrovsky Chair project ("ERA Chair at J. Heyrovský Institute of Physical Chemistry AS CR–The institutional approach towards ERA") during the finalization of the paper. The funders had no role in the preparation of the article.

Appendix A. Supplementary data

Supplementary data to this article, including literature comparison on the catalytic generation of FA, NMR spectra of new complexes and catalytic experiments can be found online at https://doi.org/10.1016/j.catcom.2020.106125.

References

[1] C. Sievers, O. Jimenez, T.E. Müller, S. Steuernagel, J.A. Lercher, Formation of solvent cages around organometallic complexes in thin films of supported ionic liquid, J. Am. Chem. Soc. 128 (2006) 13990–13991.

[2] M. Sobota, M. Happel, M. Amende, N. Paape, P. Wasserscheid, M. Laurin, J. Libuda, Ligand effects in SCILL model systems: site-specific interactions with Pt and Pd nanoparticles, Adv. Mater. 23 (2011) 2617–2621.

[3] G. La Sorella, G. Strukul, A. Scarso, Recent advances in catalysis in micellar media, Green Chem. 17 (2015) 644–683.

[4] L. Luza, C.P. Rambor, A. Gual, J.A. Fernandes, D. Eberhardt, J. Dupont, Revealing hydrogenation reaction pathways on naked gold nanoparticles, ACS Catal. 7 (2017) 2791–2799.

[5] A. Weilhard, M.I. Qadir, V. Sans, J. Dupont, Selective CO_2 hydrogenation to formic acid with multifunctional ionic liquids, ACS Catal. 8 (2018) 1628–1634.

[6] M.I. Qadir, F. Bernardi, J.D. Scholten, D.L. Baptista, J. Dupont, Synergistic CO_2 hydrogenation over bimetallic Ru/Ni nanoparticles in ionic liquids, Appl. Catal. B Environ. 252 (2019) 10–17.

[7] J. Klankermayer, S. Wesselbaum, K. Beydoun, W. Leitner, Selective catalytic synthesis using the combination of carbon dioxide and hydrogen: catalytic chess at the interface of energy and chemistry, Angew. Chem. Int. Ed. 55 (2016) 7296–7343.

[8] M.S.G. Ahlquist, Iridium catalyzed hydrogenation of CO_2 under basic conditions-mechanistic insight from theory, J. Mol. Catal. A Chem. 324 (2010) 3–8.

[9] M. Zanatta, N.M. Simon, F.P. Dos Santos, M.C. Corvo, E.J. Cabrita, J. Dupont, Correspondence on "preorganization and cooperation for highly efficient and reversible capture of low-concentration CO_2 by ionic liquids", Angew. Chem. Int. Ed. 58 (2019) 382–385.

[10] R. Tanaka, M. Yamashita, L.W. Chung, K. Morokuma, K. Nozaki, Mechanistic studies on the reversible hydrogenation of carbon dioxide catalyzed by an Ir-PNP complex, Organometallics 30 (2011) 6742–6750.

[11] T.J. Schmeier, G.E. Dobereiner, R.H. Crabtree, N. Hazari, Secondary coordination sphere interactions facilitate the insertion step in an iridium(III) CO_2 reduction catalyst, J. Am. Chem. Soc. 133 (2011) 9274–9277.

[12] C. Liu, J.-H. Xie, G.-L. Tian, W. Li, Q.-L. Zhou, Highly efficient hydrogenation of carbon dioxide to Formate catalyzed by iridium(III) complexes of imine–Diphosphine ligands, Chem. Sci. 6 (2015) 2928–2931.

[13] B. Sawatlon, M.D. Wodrich, C. Corminboeuf, Unraveling metal/pincer ligand effects in the catalytic hydrogenation of carbon dioxide to Formate, Organometallics 37 (2018) 4568–4575.

[14] E. Suárez, P. Plou, D.G. Gusev, M. Martín, E. Sola, Cationic, neutral, and anionic hydrides of iridium with PSiP pincers, Inorg. Chem. 56 (2017) 7190–7199.

[15] H. Fang, Y.-K. Choe, Y. Li, S. Shimada, Synthesis, structure, and reactivity of hydridoiridium complexes bearing a pincer-type PSiP ligand, Chem. Asian J. 6 (2011) 2512–2521.

[16] B.A. Marekha, K. Sonoda, T. Uchida, T. Tokuda, A. Idrissi, T. Takamuku, ATR-IR spectroscopic observation on intermolecular interactions in mixtures of imidazolium-based ionic liquids CnmimTFSA (n = 2–12) with DMSO, J. Mol. Liq. 232 (2017) 431–439.

[17] N.M. Simon, M. Zanatta, F.P. dos Santos, M.C. Corvo, E.J. Cabrita, J. Dupont, Carbon dioxide capture by aqueous ionic liquid solutions, ChemSusChem 10 (2017) 4927–4933.

[18] K. Rohmann, J. Kothe, M.W. Haenel, U. Englert, M. Holscher, W. Leitner, Hydrogenation of CO_2 to formic acid with a highly active ruthenium acriphos complex in DMSO and DMSO/water, Angew. Chem. Int. Ed. 55 (2016) 8966–8969.

[19] M. Zanatta, A.L. Girard, G. Marin, G. Ebeling, F.P. dos Santos, C. Valsecchi, H. Stassen, P.R. Livotto, W. Lewis, J. Dupont, Confined water in imidazolium based ionic liquids: a supramolecular guest@host complex case, Phys. Chem. Chem. Phys. 18 (2016) 18297 – 18304.

[20] S. Moret, P.J. Dyson, G. Laurenczy, Direct synthesis of formic acid from carbon dioxide by hydrogenation in acidic media, Nat. Commun. 5 (2014) 4017–4023.

[21] A. Weilhard, K. Salzmann, M. Navarro, J. Dupont, M. Albrecht, V. Sans, Catalyst design for highly efficient carbon dioxide hydrogenation to formic acid under buffering conditions, J. Catal. 385 (2020) 1–9.

[22] J.A. Laureanti, M. O'Hagan, W.J. Shaw, Chicken fat for catalysis: a scaffold is as important for molecular complexes for energy transformations as it is for enzymes in catalytic function, Sustain. Energy Fuels 3 (2019) 3260–3278.

[23] A. Chapovetsky, M. Welborn, J.M. Luna, R. Haiges, T.F. Miller, S.C. Marinescu, Pendant hydrogen-bond donors in cobalt catalysts independently enhance CO_2 reduction, ACS Cent. Sci. 4 (2018) 397–404.

[24] S.T. Ahn, E.A. Bielinski, E. Lane, Y. Chen, W.H. Bernskoetter, N. Hazari, G.T.R. Palmore, Enhanced CO_2 electroreduction efficiency through secondary coordination effects on a pincer iridium catalyst, Chem. Commun. 51 (2015) 5947–5950.

[25] S. Dey, M.E. Ahmed, A. Dey, Activation of co(I) state in a cobalt-dithiolato catalyst for selective and efficient CO_2 reduction to CO, Inorg. Chem. 57 (2018) 5939–5947.

[26] A. Alvarez, A. Bansode, A. Urakawa, A.V. Bavykina, T.A. Wezendonk, M. Makkee, J. Gascon, F. Kapteijn, Challenges in the greener production of formates/formic acid, methanol, and DME by heterogeneously catalyzed CO_2 hydrogenation processes, Chem. Rev. 117 (2017) 9804–9838.

[27] A. García-Camprubí, M. Martín, E. Sola, Addition of water across Si – Ir bonds in iridium complexes with κ-P,P,Si (biPSi) pincer ligands, Inorg. Chem. 49 (2010) 10649 – 10657.

[28] C.C. Cassol, G. Ebeling, B. Ferrera, J. Dupont, A simple and practical method for the preparation and purity determination of halide-free imidazolium ionic liquids, Adv. Synth. Catal. 348 (2006) 243–248.

[29] B. de P. Cardoso, B. Royo, M.J. Calhorda, Preference for sulfoxide S- or O-bonding to 3d transition metals – DFT insights, J. Organomet. Chem. 792 (2015) 167–176.

[30] G.B. Deacon, R.J. Phillips, Relationships between the carbon-oxygen stretching frequencies of carboxylato complexes and the type of carboxylate coordination, Coord. Chem. Rev. 33 (1980) 227–250.